Protein Crystallography under Xenon and Nitrous Oxide Pressure: Comparison with In Vivo Pharmacology Studies and Implications for the Mechanism of Inhaled Anesthetic Action

Nathalie Colloc'h,* Jana Sopkova-de Oliveira Santos,[†] Pascal Retailleau,[‡] Denis Vivarès,[§] Françoise Bonneté,[§] Béatrice Langlois d'Estainto,[¶] Bernard Gallois,[¶] Alain Brisson,[¶] Jean-Jacques Risso,[||] Marc Lemaire,** Thierry Prangé,[††] and Jacques H. Abraini*[‡‡]

*Centre CYCERON, UMR 6185, Université de Caen – CNRS, 14074 Caen cedex, France; [†]Université de Caen, UPRES-EA 2126 (CERMN)-UFR Sciences Pharmaceutiques, 14000 Caen, France; [‡]Institut de Chimie des Substances Naturelles (CNRS), 91198 Gif-sur-Yvette Cedex, France; [§]CRMCN-CNRS, Université de la Méditerranée, Marseille, France; [¶]UMR-5471 Biophysique Structurale, Université Bordeaux 1, 33405 Talence, France; [||]Institut de Médecine Navale du Service de Santé des Armées, HIA Ste-Anne, BP 610, 83800 Toulon Naval, France; **Air Liquide Research and Development, Claude-Delorme Research Centre, 78354, Jouy-en-Josas, France; [††]LCRB, UMR CNRS 8015, Faculté de Pharmacie, 75270 Paris cedex 06, France; and [‡‡]NNOXe Pharmaceuticals Inc., Québec, QC G1W 4W5, Canada

ABSTRACT   In contrast with most inhalational anesthetics, the anesthetic gases xenon (Xe) and nitrous oxide (N_2O) act by blocking the N-methyl-D-aspartate (NMDA) receptor. Using x-ray crystallography, we examined the binding characteristics of these two gases on two soluble proteins as structural models: urate oxidase, which is a prototype of a variety of intracellular globular proteins, and annexin V, which has structural and functional characteristics that allow it to be considered as a prototype for the NMDA receptor. The structure of these proteins complexed with Xe and N_2O were determined. One N_2O molecule or one Xe atom binds to the same main site in both proteins. A second subsite is observed for N_2O in each case. The gas-binding sites are always hydrophobic flexible cavities buried within the monomer. Comparison of the effects of Xe and N_2O on urate oxidase and annexin V reveals an interesting relationship with the in vivo pharmacological effects of these gases, the ratio of the gas-binding sites' volume expansion and the ratio of the narcotic potency being similar. Given these data, we propose that alterations of cytosolic globular protein functions by general anesthetics would be responsible for the early stages of anesthesia such as amnesia and hypnosis and that additional alterations of ion-channel membrane receptor functions are required for deeper effects that progress to "surgical" anesthesia.

INTRODUCTION

The mechanisms by which general anesthetics produce their action on the central nervous system are only now beginning to be discovered. This is because general anesthesia is a complex process that does not refer to one but to several physiologically altered functions. Early stages of anesthesia, such as amnesia and hypnosis, are produced at anesthetic concentrations lower than those required to produce deep sedation and reduction of motor and autonomic responses to noxious stimuli (1). The Meyer-Overton rule of a high correlation between anesthetic potency and hydrophobicity has for a long time promoted the hypothesis that anesthetics act by disrupting the structure and dynamics of lipid membranes (2). However, there is now a general consensus that general anesthetics act by disrupting protein functions (3,4). Even if general anesthetics have been shown to interact with globular proteins in a manner consistent with the Meyer-Overton rule (5,6), the proteins considered as their most likely molecular targets at clinically relevant concentrations are ion-channel receptors (4,7). The current opinion is that general anesthetics act by enhancing the activity of inhibitory receptors and by inhibiting the activity of excitatory receptors (1). The main target of most inhalational anesthetics is considered to be the γ-amino-butyric acid type A (GABA$_A$) inhibitory receptor (8–10). In contrast, xenon (Xe) and nitrous oxide (N_2O), which are gaseous anesthetics, are most efficient against the N-methyl-D-aspartate (NMDA) excitatory receptor and to a lesser extent against the neuronal nicotinic receptor and the TREK-1 two-pore K^+ channel (11–14). In addition, it should be mentioned that a recent study has identified the existence of a specific gas channel that may serve to accelerate gas action (15), but the relevance of this finding to general anesthesia still remains to be demonstrated.

Scales that assess the in vivo potency of inhaled anesthetics in humans are based on the minimum alveolar anesthetic concentrations (MAC) that are associated with well-defined behavioral endpoints. For example, MAC-awake defines the MAC that prevents voluntary responses to spoken commands, i.e., the impairment of perceptive awareness to environmental stimuli (hypnosis), and MAC-immobility defines the MAC that produces deep sedation and suppresses purposeful movement in response to a standard noxious stimulus (1). Likewise, laboratory animals can be assessed for MAC-immobility. Although MAC-awake can, in the strict sense, be measured only in humans, anesthetic-induced loss of the righting reflex in animals is considered a

behavioral endpoint for which the dependence on anesthetic concentration is closely related to MAC-awake (1).

Although the potency of inhalational anesthetics is usually in accord with the Meyer-Overton rule, there are a number of alterations and exceptions that emphasize the complexity of the molecular routes through which these anesthetic compounds act. For example, the so-called nonimmobilizers, which are large halogenated alkanes predicted to be potent anesthetics by the Meyer-Overton rule, produce amnesia but lack of immobilizing activity (16). And whereas the ratio of MAC-awake for N_2O and Xe is ~1.4 (17–19), with respect to the Meyer-Overton rule, the ratio of MAC-immobility for these gases is only 1 (19–22). Then, it is likely that the early stages of anesthesia and the deeper effects that progress to ''surgical'' anesthesia are mediated by separate sites and mechanisms (23,24).

With plausible inhalational anesthetic targets now identified, current investigations attempt to determine which targets are actually responsible for the different and multiple stages of anesthesia. Unfortunately, at the structural biology level, no one structure is known today for proteins thought to be anesthetic targets. Structural investigations on particular soluble proteins chosen as close models may be an approach to understand the binding mode of inhalational anesthetics and to appreciate the molecular changes that these gases produce on their targets (21).

To identify and compare the binding characteristics of N_2O and Xe, we performed x-ray crystallography studies on two structural models, urate oxidase and annexin V. Urate oxidase is a prototype of a variety of intracellular globular proteins that possess large hydrophobic cavities (25). Annexin V is a protein that binds to biological membranes in a reversible calcium-dependent manner and possesses a hydrophilic pore, believed to be the calcium conduction pathway, that lies at the interface of four homologous and structurally related domains (26). These structural characteristics and functional properties of ion selectivity and voltage gating allow annexin V to be considered as a prototype for the NMDA receptor (27,28). Xe, but not N_2O, binding ability to urate oxidase has already been studied (29). No structure of annexin V with gas has ever been solved before. Although argon and krypton have been shown to bind to the same site as Xe in two examples of globular proteins (30,31), our investigations in urate oxidase and annexin V were restricted to Xe and N_2O, which mainly act by inhibiting the NMDA receptor (11–13) because argon and krypton do not seem to exert their effect through this receptor (32,33). In a recent study, Miller indicated that the gas pressure for crystallography studies should be at least 10 times higher than their physiological concentration to approximate binding saturation (24). In the study presented here, we identified discrete binding sites for Xe and N_2O at 2 MPa (or 20 bar) and further demonstrated that the gas-binding cavities' expansion ratios in urate oxidase and annexin V are consistent with the in vivo physiological effects of these gases.

MATERIALS AND METHODS

Crystals of *Aspergillus flavus* urate oxidase, a tetrameric peroxisomal protein of 135 kDa, complexed with its inhibitor, 8-azaxanthin, and crystals of rat annexin V, a trimeric protein of 105 kDa, in high calcium concentration were grown as described previously (34,35). The method used to prepare Xe complexes has been described earlier (36). N_2O complexes were prepared similarly. Native crystal, mounted in a quartz capillary, fitted to a specially designed cell, was submitted to gas pressure a few minutes before the start of data collection. A gas pressure of 2 MPa was maintained during the data collection. Diffraction data were collected at the DW32 wiggler beam line at the LURE synchrotron facility in Orsay, France, using x-rays at a wavelength of 0.964 Å and a 345-mm MAR-Research image plate detector, and at the ESRF (Grenoble, France) BM14 beamline, at a wavelength of 0.972 Å and operating in a 16-bunch mode, using a MAR CCD detector; temperature was set to 277 K in all cases. Data were integrated by *DENZO* and scaled independently using *SCALEPACK*, both programs from the *HKL* package (37). Data reduction and reindexing when necessary were carried out with programs of the *CCP4* package (38). Structure refinements were carried out by *REFMAC* from the *CCP4* package (39). The starting model for urate oxidase rigid body refinement was the PDB entry 1R51 (resolution 1.75 Å) (40), and the starting model for annexin V refinement was the PDB entry 1A8A (resolution 1.90 Å) (41). In all cases, solvent, ion, and/or inhibitor molecules were removed from the original model. The graphic program *O* (42) was used to visualize the 2*Fobs-Fcalc* and the *Fobs-Fcalc* electron-density maps and for manual rebuilding. A summary of the data collections and refinement parameters is shown in Table 1. The gas complexes have been compared to the native structures collected in parallel. Cavity volumes were calculated with the program *VOIDOO* (43). The following parameters gave the most reliable results for both proteins with the lowest mean deviation: primary grid spacing, 0.6 Å; grid spacing, 0.6 Å; probe radius, 1.0 Å. Slightly different results were obtained when different orientations of the model were used. Thus, the accuracy of cavity volume calculations and the mean deviation were estimated by repeating the calculations on nine randomly oriented copies of the model. To check whether the cavity volume expansion ratios are dependent or not on the methods used, the different structures were also refined in parallel with *SHELXL* from the *SHELX-97* package (44), and cavities' volumes were similarly calculated using the program *CASTp* (45) with a probe radius of 1.3 Å for a reliable estimation of the cavity volume.

RESULTS

The four complexes studied (urate oxidase with Xe and N_2O and annexin V with Xe and N_2O) were solved at a resolution better than 1.75 Å, allowing unambiguous detection of the bound gas (Fig. 1). The complex urate oxidase-Xe has already been solved, but at a lower resolution because Xe has been used as a heavy atom derivative for the initial structure resolution (25). It was shown that Xe binds to urate oxidase in a unique site with an occupancy factor sufficient to solve the structure. It is confirmed in this case that Xe is located at the same place, just behind the active site, with an occupancy evaluated at ~0.9 (Fig. 1 *A*). In the case of annexin V, it was the first time that a complex with Xe was analyzed. Xe binds to a unique site, a hydrophobic cavity located in the center of the third domain, with an occupation factor of ~0.4 (Fig. 1 *C*). In these two proteins, Xe binds to a preexisting hydrophobic flexible gas cavity buried within the monomer with no visible water. No structural studies of proteins with N_2O have been reported until the investigation presented

TABLE 1 Crystallographic data collections and refinement statistics

Protein	Urate oxidase			Annexin V		
Gas	–	Xe	N_2O	–	Xe	N_2O
Data collection						
Space group	I222	I222	I222	H3	H3	H3
Unit cell parameters (Å)						
a	80.49	80.50	80.19	156.98	156.99	157.03
b	96.04	96.58	96.03	156.98	156.99	157.03
c	105.34	106.01	105.21	37.48	37.34	37.33
Resolution range (Å)	50–1.5	20–1.75	70–1.75	78–1.74	78–1.83	78–1.74
Unique reflections	59653	34588	41239	32838	25958	34281
(Final shell)	(5710)	(1813)	(4076)	(3387)	(2674)	(2953)
Overall R_{sym}*(%)	5.6	4.9	5.5	4.6	5.1	4.5
(Final shell)	(27.1)	(5.3)	(34.6)	(20.2)	(25.8)	(17.8)
Completeness (%)	91.1	82.5	99.9	92.9	85.8	97.3
(Final shell)	(87.9)	(44.3)	(99.8)	(95.5)	(88.3)	(83.2)
Refinement statistics (REFMAC)						
Resolution range	20–1.5	20–1.7	20–1.7	20–1.7	20–1.8	20–1.7
R_{value}[†](%)	17.63	16.72	16.29	17.04	16.78	17.39
R_{free}[‡](%)	19.77	19.94	18.56	19.24	19.85	20.19
$\langle B \rangle$ for protein atoms[§]($Å^2$)	19.89	20.05	21.97	25.68	27.13	29.21
$\langle B \rangle$ for waters[¶]($Å^2$)	31.98	30.33	34.70	34.03	33.47	37.26
Weighted rmsd from ideality						
Bond length (Å)	0.010	0.014	0.013	0.012	0.013	0.013
Bond angle (°)	1.41	1.50	1.60	1.43	1.47	1.47
PDB code	2IBA	2IC0	2ICQ	–	2IE6	2IE7

*R_{sym} is defined as $\sum_{h,k,l} \sum_i |I_i(h, k, l) - I_i(h, k, l)| / \sum_{h,k,l} \sum_i I_i(h, k, l)$ where $I_i(h,k,l)$ is the ith observation of reflection h,k,l and $\langle I(h,k,l) \rangle$ is the weighted mean of all observations (after rejection of outliers).

[†]R_{value} is defined as $\sum |F_o| - |F_c| / \sum |F_o|$ and indicates the accuracy of the model.

[‡]R_{free} is a cross validation residual calculated using 10% of the native data, which were randomly chosen and excluded from the refinement.

[§]Includes inhibitor atoms for urate oxidase.

[¶]Includes gas for urate oxidase and includes calcium ion, sulfate ion, and gas for annexin V.

here, to our knowledge. N_2O binds to urate oxidase in the same cavity as Xe, with a lower occupation factor of ~0.7 (Fig. 1 *B*). N_2O also binds to annexin V in the same site as Xe, but with a higher occupation factor evaluated at ~0.9 (Fig. 1 *D*). Thus, in the two proteins, a molecule of N_2O is found exactly at the same location as the Xe atom, showing that N_2O shares some physicochemical properties with Xe. However, in both proteins, a second N_2O molecule is observed. In urate oxidase, this second molecule is found within the same hydrophobic cavity, orthogonally oriented with respect to the first one, with a lower occupation factor of ~0.6 (Fig. 1 *B*). In annexin V, the second molecule, with an occupation factor of 0.7, is found in another hydrophobic cavity located in the center of the first domain (Fig. 1 *E*). In the annexin V-Xe complex, this cavity is empty. In all cases, the bound gas is surrounded by five or six side-chain carbon atoms from aliphatic residues at <4.5 Å for the Xe atom and at <4.0 Å for the two N_2O molecules (Table 2). The overall protein structures showed, as expected, very little perturbation on gas binding, with an overall root mean-square deviation <0.15 Å for the backbone and <0.40 Å for all protein atoms. However, contrary to what was expected (pressure should lead to a volume compression), both Xe and N_2O produce a volume expansion of the cavities where they

bind, resulting from slight displacements of the side chain atoms lining the cavities.

In urate oxidase, Xe induces a volume increase of 23.5%. Matthews and co-workers (30) found a similar expansion effect of Xe in the globular phage T4 lysozyme structure. N_2O induces a volume expansion of 17.9%, leading to a ratio of volume expansion for Xe and N_2O of 1.32 (Table 3). Equivalent ratio values are obtained when the structures are independently refined with *SHELXL* instead of *REFMAC* (ratio of 1.44), cavity volumes calculated with *CASTp* instead of *VOIDOO* (ratio of 1.51), or *SHELXL* and *CASTp* used simultaneously (ratio of 1.25), thereby leading to an average ratio of volume expansion of 1.38 (data not shown).

In annexin V, Xe and N_2O respectively induce volume expansions of their primary binding site of 14.1% and 32.1%, leading to a ratio of volume expansion for Xe and N_2O of 0.44 (Table 3). Equivalent ratio values are obtained when the structures are independently refined with *SHELXL* instead of *REFMAC* (ratio of 0.58), cavity volumes calculated with *CASTp* instead of *VOIDOO* (ratio of 0.46), or *SHELXL* and *CASTp* used simultaneously (ratio of 0.36), thereby leading to an average ratio of volume expansion of 0.46 (data not shown); in addition, N_2O also expands the volume of its secondary binding site by 33.0% (Table 3).
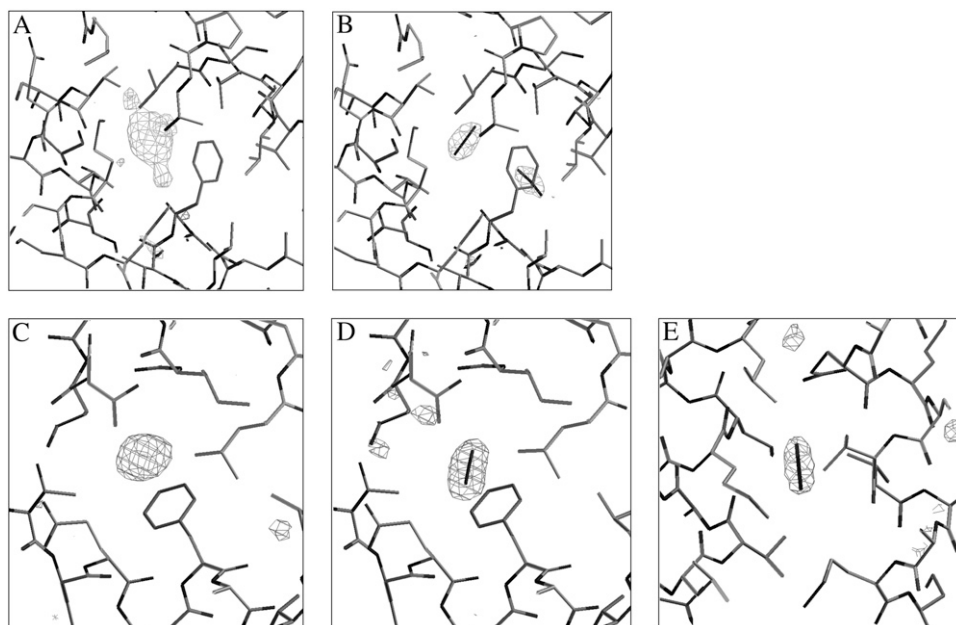
FIGURE 1 Omit maps of the two gases within the two proteins. Omit maps showing the position of the Xe atom (*A*) or of the two N_2O molecules (*B*) within urate oxidase binding site cavity. Omit maps showing the position of the Xe atom (*C*), the first N_2O molecule (*D*), and the second N_2O molecule (*E*) in annexin V. (Contour levels at 3 SD above the average background.)

When we consider the effects of Xe and N_2O on urate oxidase and annexin V together as a model of simultaneous occupation of cytosolic and membrane proteins by Xe or N_2O (see the discussion section about the implications for general anesthesia mechanisms), we find an overall expansion of the gas-binding cavities of 20.6% in presence of Xe and of 22.2% in presence of N_2O, leading to an expansion ratio of 0.93 (Table 3). Equivalent ratio values are obtained when the structures are independently refined with *SHELXL* instead of *REFMAC* (ratio of 1.14), cavity volumes calcu-

lated with *CASTp* instead of *VOIDOO* (ratio of 1.09), or *SHELXL* and *CASTp* used simultaneously (ratio of 0.96), thereby leading to an average ratio of volume expansion of 1.03 (data not shown).

DISCUSSION

Many Xe-protein complexes have been solved, showing that Xe atoms bind not only to intramolecular cavities but also to intermolecular sites or exposed pockets (29,46). However, in the majority of cases, Xe binds to inaccessible hydrophobic preexisting flexible gas cavities. Here, we show that the primary binding sites of Xe and N_2O within two soluble proteins, urate oxidase and annexin V, are identical flexible gas cavities with no visible water. Even if the pressure used is higher than any physiological pressure used in anesthesia because of the x-ray crystallography technique, which needs an elevated gas pressure to saturate the site for direct observation (24), we can draw the hypothesis that these two gases would bind to the same site within their main physiological target, the pore of the NMDA receptor. We chose to study these gases at a same pressure of 2 MPa for a more rational comparison of their effects.

Implication for protein function

Internal cavities within proteins are crucial for conformational flexibility and domain motion (47,48) and thereby for protein and cell functions. A ligand can reach a buried cavity through thermal motion (49). It was proposed that only proteins with large enough preexisting internal cavities can bind anesthetics (30). Occupation and expansion of large hydrophobic flexible gas cavities within intracellular or membrane

TABLE 2 Closest contacts (in Å) around the xenon atom (Xe), the nitrous oxide molecule (N_2O (1)) located at the same position as the Xe atom and the second nitrous oxide molecule (N_2O (2)) in urate oxidase (see Fig. 2) and annexin V (see Fig. 3)

	Urate oxidase				Annexin V		
Xe	3.91	Cδ2	Leu-252	Xe	2.93	Cγ2	Thr-227
	3.95	Cδ2	Leu-252		3.65	Cδ2	Phe-192
	4.09	Cδ1	Phe-219		3.86	Cδ1	Leu-235
	4.29	Cδ2	Leu-178		3.90	Cγ2	Thr-287
	4.30	Cγ1	Val-227		3.99	Cβ	Glu-226
	4.43	Cε	Met-234				
N_2O (1)	3.25	Cγ2	Thr-230	N_2O (1)	3.23	Cγ2	Thr-227
	3.50	Cγ	Thr-180		3.42	Cγ	Phe-192
	3.52	Cδ2	Leu-178		3.49	Cδ1	Leu-235
	3.59	Cδ	Leu-252		3.65	Cγ2	Thr-187
	3.77	Cγ1	Val-227		3.85	Cβ	Glu-223
	3.81	Cε1	Phe-219				
N_2O (2)	3.19	Cβ	Phe-219	N_2O (2)	3.32	Cγ2	Val-80
	3.32	Cγ2	Thr-215		3.36	Cγ1	Val-64
	3.33	Cγ2	Val-182		3.43	Cβ	Met-67
	3.50	Cε	Met-234		3.51	Cγ2	Ile-79
	3.50	Cγ2	Thr-180		3.75	O	Glu-76
					3.83	Cδ1	Leu-71

TABLE 3 Cavities volume (calculated with *VOIDOO* (43)) for urate oxidase and annexin V (refined with *REFMAC* (39)) with their mean deviation, expansion for xenon (Xe) and nitrous oxide (N$_2$O) binding sites and ratio of expansion.

Protein	Cavity volume $\pm$ mean deviation (Å^3)	Volume expansion (%)	Expansion ratio (Xe/N$_2$O)
Urate oxidase			
Cavity 1	119.1 $\pm$ 2.0		
+ Xe	147.1 $\pm$ 2.5	23.5	
+ N$_2$O	140.3 $\pm$ 2.9	17.9	1.32*
Annexin V			
Cavity 1	52.9 $\pm$ 1.5		
+ Xe	60.4 $\pm$ 1.1	14.1	
+ N$_2$O	69.9 $\pm$ 2.0	32.1	0.44
Cavity 2	31.1 $\pm$ 1.4		
+ N$_2$O	41.4 $\pm$ 1.1	33.0	–
Cavities 1 + 2	84.0 $\pm$ 2.9		
+ N$_2$O	111.3 $\pm$ 3.1	32.4	0.44[†]
Urate oxidase + annexin V			
Cavities 1	172.0 $\pm$ 3.4		
+ Xe	207.5 $\pm$ 3.6	20.6	
+ N$_2$O	210.2 $\pm$ 4.9	22.2	0.93[‡]
Cavities 1 + 2	203.1 $\pm$ 4.9		
+ N$_2$O	251.6 $\pm$ 6.0	23.9	0.86[†]

*In accord with the relative narcotic potency of Xe compared to N$_2$O when assessed by loss of the righting reflex, a behavioral endpoint whose dependence on anesthetic concentration is closely related to MAC-awake (see Table 4).

[†]Compared to expansion induced by Xe.

[‡]In accord with the relative anesthetic potency of Xe compared to N$_2$O when assessed by lack of purposeful movement in response to a noxious stimulus, an endpoint that allows defining MAC-immobility values (see Table 4). Equivalent expansion ratio values are obtained when the structures are independently refined with *SHELXL* instead of *REFMAC*, cavity volumes calculated with *CASTp* instead of *VOIDOO*, or *SHELXL* and *CASTp* used simultaneously.

FIGURE 2 Urate oxidase binding sites for Xe or N$_2$O. Smooth carbon α-chain representation of urate oxidase monomer with the hydrophobic gas-binding site at close proximity to the active site pocket occupied by the competitive inhibitor 8-azaxanthin. One atom of Xe or two N$_2$O molecules bind within the hydrophobic cavity. Oxygen, nitrogen, and Xe atoms are colored in red, blue, and orange, respectively.

proteins may therefore lead to conformational rigidity, thereby disrupting protein and cell functions. In urate oxidase, we found that the gas-binding cavity is situated near the active site where the competitive inhibitor, 8-azaxanthin, binds (Fig. 2). It is then plausible that occupation and expansion by Xe or N$_2$O of this large hydrophobic gas-binding cavity may restrain or disrupt the catalytic activity of urate oxidase. As regards annexin V, the native structure is known at high and low calcium concentration (35,50), showing a calcium-induced large-scale conformational movement within the third domain of the protein. The loop carrying a tryptophan residue buried within the core of this domain moves, making the tryptophan solvent-accessible and ready to bind to membrane lipids. In parallel, a glutamate residue switches to a position where it is ready to bind the calcium ion (Fig. 3). This hinge movement, believed to open the calcium ion path, is a key step for the protein fixation to and detachment from the membrane and all its functional roles (51,52). In the annexin-gas complexes solved here at high
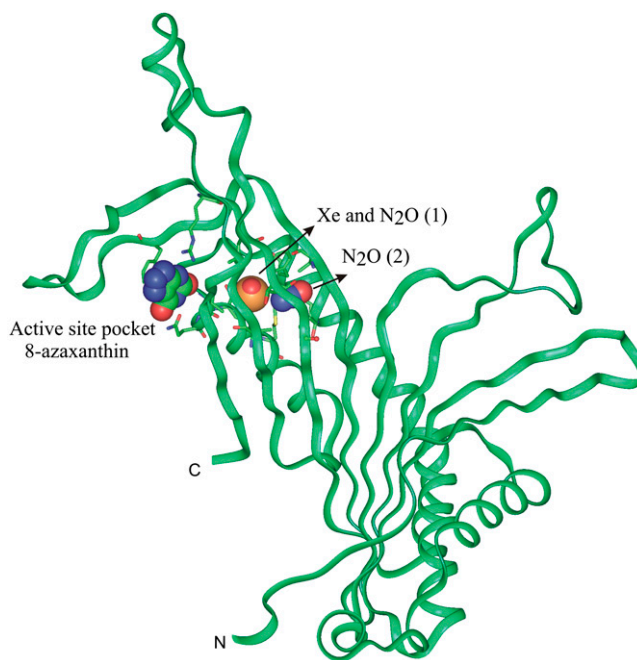
calcium concentration, both Xe and N$_2$O bind within the hydrophobic cavity left vacant by the outer solvent-accessible position of the tryptophan. It is then plausible that occupation and expansion of this cavity by Xe and N$_2$O would prohibit the hinge movement of the loop necessary for all annexin V functions, thereby disrupting them. These findings and their plausible consequences on protein functioning are in agreement with previous experiments showing that binding of anesthetics leads to an increase in protein stability (53) and to a reduction of kinetics in single nicotinic acetylcholine channels (54). This receptor possesses a structure close to that of the NMDA ion-channel receptor, which is known to be a main target for Xe and N$_2$O (11–13). By analogy, we suggest that the presence of a gas bound to a hydrophobic cavity within the transmembrane domain of the NMDA receptor channel, as shown for the nicotinic acetylcholine receptor channel (55), may alter the flexibility of the pore, thereby limiting calcium exchange and disrupting the NMDA receptor function. Interestingly, we found that Xe and N$_2$O bind to a same site in the center of the third domain of annexin V and that N$_2$O also binds to a second cavity located in the center of the first annexin V domain. This may be related to recent pharmacological findings that have suggested that N$_2$O may interact with both the NR1 and NR2D subunits of the NMDA receptor (56,57), whereas Xe may act only at the NR2D subunit (57,58).
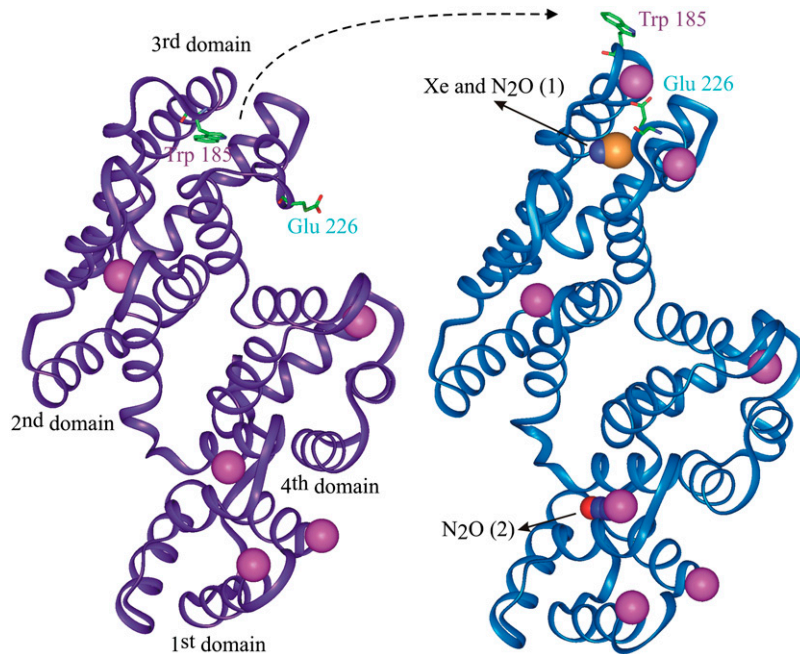
FIGURE 3   Annexin V hinge movement and binding sites of Xe or N_2O. Smooth carbon α-chain representation of annexin V monomer in low- and high-calcium conformation (*colored* in *purple* and *blue*, respectively) showing the hinge movement of the loop carrying the tryptophan 185 in parallel to the glutamate 226 switch. Both Xe and N_2O bind within the hydrophobic cavity left vacant by the movement of the tryptophan. A second molecule of N_2O binds in the center of the first domain. The color code is the same as above plus the calcium colored in pink. Figs. 2 and 3 were produced with the visualization software InsightII (Accelrys, San Diego, CA).

Implication for the mechanisms of general anesthesia

The range and average value of the volume expansion ratio of the gas-binding cavities for Xe and N_2O in urate oxidase (range 1.25–1.51, mean 1.38) fit both with the Meyer-Overton concept and the ratio of the in vivo effects of these gases when assessed by the loss of the righting reflex (range 1.28–1.49, mean 1.38; see Table 4), a behavioral endpoint whose dependence on anesthetic concentration is closely related to MAC-awake (1). This indicates that the concordance

between the volume expansion effects of Xe and N_2O and the in vivo MAC-awake effects of these gases is between 97.5% (1.25:1.28) and 98.5% (1.49:1.51). No similar relationship is found for annexin V. However, we found that the range and average value of the volume expansion ratio of the gas-binding cavities for Xe and N_2O in urate oxidase and annexin V, taken together as a model of simultaneous occupation of cytosolic and membrane proteins (range 0.93–1.14, mean 1.03), do fit with the ratio of the in vivo effects of these gases when assessed by the absence of purposeful movement in response to noxious stimuli (range 0.95–0.99, mean 0.97; see Table 4), an endpoint that defines MAC-immobility values (1). This indicates that the concordance between the volume expansion effects of Xe and N_2O and the in vivo MAC-immobility effects of these gases is between 87% (0.99:1.14) and 98% (0.93:0.95). Whenever such effects occur in brain cytosolic and membrane receptors, they may be of physiological significance and may help to reconcile the critical volume expansion theory, initially developed for membrane lipids, with protein theories of anesthesia (59).

Based on the data of the study presented here, we hypothesize a step-by-step mechanism of inhaled anesthetic action in which the graded dose-response effect would depend on cavity size and order of filling. Xe and N_2O would first bind to brain intracellular proteins possessing large hydrophobic cavities, which constitute easy targets for inhalational anesthetics, thereby disrupting the activity of these proteins in a manner sufficient to induce moderate neuronal dysfunctions leading to the early stages of anesthesia, i.e., amnesia and hypnosis. If gas concentration rises, the smaller hydrophobic gas-binding cavities within the NMDA receptor would then begin to be filled (with the cytosolic protein-binding cavities

TABLE 4   Mean anesthetic concentration (MAC) of xenon (Xe) and nitrous oxide (N_2O) producing loss of righting reflex and lack of response to noxious stimuli in rodents (references in parentheses)

Behavioral endpoint	MAC value (vol %)	Average MAC (vol %)	Mean relative Narcotic potency*
Loss of righting reflex (MAC-awake)			
N_2O	128 (17)	125	
	122 (18)		
Xe	86 (17)	90.5	1.38
	95 (19)		
Lack of response to noxious stimuli (MAC-immobility)			
N_2O	153,158 (20)		
	155 (21)	156	
	159 (22)		
Xe	161 (19)	161	0.97

*The relative anesthetic potency of Xe is expressed compared to the anesthetic potency of N_2O taken as a 100% value. The relative narcotic potencies of Xe and N_2O calculated from the different experimental MAC-awake and MAC-immobility values range from 1.28 to 1.49 (mean value 1.38) and from 0.95 to 0.99 (mean value 0.97), respectively.

still fully occupied), thereby disrupting the receptor function and leading to surgical anesthesia, i.e., deep sedation and lack of autonomic and motor responses to noxious stimuli. Similar step-by-step mechanisms of general anesthesia, which assume a causal link between the behavioral effects of anesthesia from amnesia and hypnosis to ''surgical anesthesia'' and the progressive occupation of the anesthetic binding sites from globular proteins to ion channel receptors, may occur for other types of inhaled anesthetics and/or ion-channel receptors, such as the $GABA_A$ receptor, which is thought to be the molecular target of most volatile anesthetics (8–10). Such mechanisms may also explain a number of critical exceptions to the Meyer-Overton rule of a high correlation between anesthetic potency and hydrophobicity, depending on the relative size of the anesthetics and of the anesthetic-binding cavities within ion channel receptors. For instance, the so-called nonimmobilizers, predicted to be potent anesthetics by the Meyer-Overton rule, produce amnesia but lack of immobilizing activity (16). According to our model, the large size of the so-called nonimmobilizers may allow these gases to bind to cytosolic globular proteins but not to ion channel receptors, which possess smaller hydrophobic cavities, thereby producing moderate neuronal dysfunction and leading to the production of amnesia but not to immobilizing activity.

REFERENCES

1. Campagna, J. A., K. W. Miller, and S. A. Forman. 2003. Mechanisms of actions of inhaled anesthetics. *N. Engl. J. Med.* 348:2110–2124.

2. Janoff, A. S., M. J. Pringle, and K. W. Miller. 1981. Correlation of general anesthetic potency with solubility in membranes. *Biochim. Biophys. Acta.* 649:125–128.

3. Franks, N. P., and W. R. Lieb. 1984. Do general anaesthetics act by competitive binding to specific receptors? *Nature.* 310:599–601.

4. Franks, N. P., and W. R. Lieb. 1994. Molecular and cellular mechanisms of general anaesthesia. *Nature.* 367:607–614.

5. Slater, S. J., K. J. A. Cox, J. V. Lombardi, C. Ho, M. B. Keily, E. Rubin, and C. D. Stubbs. 1993. Inhibition of protein kinase C by alcohols and anaesthetics. *Nature.* 364:82–84.

6. Hemmings, H. C., Jr., and A. I. Adamo. 1994. Effects of halothane and propofol on purified brain protein kinase C activation. *Anesthesiology.* 81:147–155.

7. Narahashi, T., G. L. Aistrup, J. M. Lindstrom, W. Marszalec, K. Nagata, F. Wang, and J. Z. Yeh. 1998. Ion channel modulation as the basis for general anesthesia. *Toxicol. Lett.* 100–101:185–191.

8. Krasowski, M. D., and N. L. Harrison. 1999. General anaesthetic actions on ligand-gated ion channels. *Cell. Mol. Life Sci.* 55:1278–1303.

9. Quinlan, J. J., G. E. Homanics, and L. L. Firestone. 1998. Anesthesia sensitivity in mice that lack the beta3 subunit of the gamma-aminobutyric acid type A receptor. *Anesthesiology.* 88:775–780.

10. Sonner, J. M., M. Cascio, Y. Xing, M. S. Fanselow, J. E. Kralic, A. L. Morrow, E. R. Korpi, S. Hardy, B. Sloat, E. I. Eger 2nd, and G. E. Homanics. 2005. Alpha 1 subunit-containing GABA type A receptors in forebrain contribute to the effect of inhaled anesthetics on conditioned fear. *Mol. Pharmacol.* 68:61–68.

11. Franks, N. P., R. Dickinson, S. L. de Sousa, A. C. Hall, and W. R. Lieb. 1998. How does xenon produce anaesthesia? *Nature.* 396:324.

12. Jevtovic-Todorovic, V., S. M. Todorovic, S. Mennerick, S. Powell, K. Dikranian, N. Benshoff, C. F. Zorumski, and J. W. Olney. 1998. Nitrous oxide (laughing gas) is an NMDA antagonist, neuroprotectant and neurotoxin. *Nat. Med.* 4:460–463.

13. Yamakura, T., and R. A. Harris. 2000. Effects of gaseous anesthetics nitrous oxide and xenon on ligand-gated ion channels. Comparison with isoflurane and ethanol. *Anesthesiol.* 93:1095–1101.

14. Gruss, M., T. J. Bushell, D. P. Bright, W. R. Lieb, A. Mathie, and N. P. Franks. 2004. Two-pore-domain K^+ channels are a novel target for the anesthetic gases xenon, nitrous oxide, and cyclopropane. *Mol. Pharmacol.* 65:443–452.

15. Khademi, S., J. O'Connell III, J. Remis, Y. Robles-Colmenares, L. J. W. Miercke, and R. M. Stroud. 2004. Mechanism of ammonia transport by Amt/MEP/Rh: structure of AmtB at 1.35 Å. *Science.* 305:1587–1594.

16. Kandel, L., B. S. Chortkoff, J. Sonner, M. J. Laster, and E. I. Eger II. 1996. Nonanesthetics can suppress learning. *Anesth. Analg.* 82:321–326.

17. David, H. N., F. Leveillé, L. Chazalviel, E. T. MacKenzie, A. Buisson, M. Lemaire, and J. H. Abraini. 2003. Reduction of ischemic brain damage by nitrous oxide and xenon. *J. Cereb. Blood Flow Metab.* 23:1168–1173.

18. Miller, K. W., M. W. Wilson, and R. A. Smith. 1978. Pressure resolves two sites of action of inert gases. *Mol. Pharmacol.* 14:950–959.

19. Koblin, D. D., Z. Fang, E. I. Eger II, M. J. Laster, D. Gong, P. Ionescu, M. J. Halsey, and J. R. Trudell. 1998. Minimum alveolar concentrations of noble gases, nitrogen, and sulfur hexafluoride in rats: helium and neon as nonimmobilizers (nonanesthetics). *Anesth. Analg.* 87:419–424.

20. Russell, G. B., and J. M. Graybeal. 1992. Direct measurement of nitrous oxide MAC and neurologic monitoring in rats during anesthesia under hyperbaric conditions. *Anesth. Analg.* 75:995–999.

21. Russell, G. B., and J. M. Graybeal. 1995. Differences in anesthetic potency between Sprague-Dawley and Long-Evans rats for isoflurane but not nitrous oxide. *Pharmacology.* 50:162–167.

22. Russell, G. B., and J. M. Graybeal. 1998. Nonlinear additivity of nitrous oxide and isoflurane potencies in rats. *Can. J. Anaesth.* 45:466–470.

23. Eger II, E. I., D. D. Koblin, R. A. Harris, J. J. Kendig, A. Pohorille, M. J. Halsey, and J. R. Trudell. 1997. Hypothesis: inhaled anesthetics produce immobility and amnesia by different mechanisms at different sites. *Anesth. Analg.* 84:915–918.

24. Miller, K. W. 2002. The nature of sites of general anaesthetic action. *Br. J. Anaesth.* 89:17–31.

25. Colloc'h, N., M. El Hajji, B. Bachet, G. L'Hermite, M. Schiltz, T. Prangé, B. Castro, and J. P. Mornon. 1997. Crystal structure of the protein drug urate oxidase-inhibitor complex at 2.05 Å resolution. *Nat. Struc. Biol.* 4:947–952.

26. Gerke, V., and S. E. Moss. 2002. Annexins: from structure to function. *Physiol. Rev.* 82:331–371.

27. Berendes, R., D. Voges, P. Demange, R. Huber, and A. Burger. 1993. Structure-function analysis of the ion channel selectivity filter in human annexin V. *Science.* 262:427–430.

28. Demange, P., D. Voges, J. Benz, S. Liemann, P. Göttig, R. Berendes, A. Burger, and R. Huber. 1994. Annexin V: the key to understanding ion selectivity and voltage regulation? *Trends Biochem. Sci.* 19:272–276.

29. Prangé, T., M. Schiltz, L. Pernot, N. Colloc'h, S. Longhi, W. Bourguet, and R. Fourme. 1998. Exploring hydrophobic sites in proteins with xenon or krypton. *Proteins*. 30:61–73.

30. Quillin, M. L., W. A. Breyer, I. J. Griswold, and B. W. Matthews. 2000. Size versus polarizability in protein-ligand interactions: binding of noble gases within engineered cavities in phage T4 lysozyme. *J. Mol. Biol.* 302:955–977.

31. Schiltz, M., R. Fourme, and T. Prangé. 2003. Use of noble gases xenon and krypton as heavy atoms in protein structure determination. *Methods Enzymol.* 374:83–119.

32. Abraini, J. H. 2001. Etude des Paramètres Cinétiques des Gaz Inertes: Azote, Argon, Krypton, Protoxyde d'Azote et Xénon.: Air Liquide Santé International, Paris, France.

33. Abraini, J. H., B. Kriem, N. Balon, J. C. Rostain, and J. J. Risso. 2003. Gamma-aminobutyric acid neuropharmacological investigations on narcosis produced by nitrogen, argon, or nitrous oxide. *Anesth. Analg.* 96:746–749.

34. Bonneté, F., D. Vivarès, C. Robert, and N. Colloc'h. 2001. Interactions in solution and crystallization of *Aspergillus flavus* urate oxidase. *J. Crystal Growth*. 232:330–339.

35. Sopkova, J., M. Renouard, and A. Lewit-Bentley. 1993. The crystal structure of a new high-calcium form of annexin V. *J. Mol. Biol.* 234:816–825.

36. Schiltz, M., T. Prangé, and R. Fourme. 1994. On the preparation and x-ray data collection of isomorphous xenon derivatives. *J. Appl. Crystallogr.* 27:950–960.

37. Otwinowski, Z., and W. Minor. 1997. Processing of x-ray diffraction data collected in the oscillation mode. *Methods Enzymol.* 276:307–326.

38. Collaborative Computational Project, N. 1994. The *CCP4* suite: programs for protein crystallography. *Acta Crystallogr.* D50:760–763.

39. Murshudov, G. N., A. A. Vagin, and E. J. Dodson. 1997. Refinement of macromolecular structures by the Maximum-Likelihood method. *Acta Crystallogr.* D53:240–255.

40. Retailleau, P., N. Colloc'h, D. Vivarès, F. Bonneté, B. Castro, M. El Hajji, J. P. Mornon, G. Monard, and T. Prangé. 2004. Complexed and ligand-free high-resolution structures of urate oxidase (Uox) from *Aspergillus flavus*: a reassignment of the active-site binding mode. *Acta Cryst.* D60:453–462.

41. Swairjo, M. A., N. O. Concha, M. A. Kaetzel, J. R. Dedman, and B. A. Seaton. 1995. $Ca^{(2+)}$-bridging mechanism and phospholipid head group recognition in the membrane-binding protein annexin V. *Nat. Struct. Biol.* 2:968–974.

42. Jones, T. A., J. Y. Zou, S. W. Cowan, and M. Kjeldgaard. 1991. Improved methods for building protein models in electron density maps and the location of errors in these models. *Acta Crystallogr.* A47:110–119.

43. Kleywegt, G. J., and T. A. Jones. 1994. Detection, delineation, measurement and display of cavities in macromolecular structures. *Acta Crystallogr.* D50:178–185.

44. Sheldrick, G. M., and T. R. Schneider. 1997. SHELXL: High-resolution refinement. *Methods Enzymol.* 227:319–343.

45. Binkowski, T. A., S. Naghibzadeh, and J. Liang. 2003. CASTp: Computed Atlas of Surface Topography of proteins. *Nucleic Acids Res.* 31:3352–3355.

46. Sauer, O., M. Roth, T. Schirmer, G. Rummel, and C. Kratky. 2002. Low-resolution detergent tracing in protein crystals using xenon or krypton to enhance x-ray contrast. *Acta Crystallogr.* D58:60–69.

47. Hubbard, S. J., K. H. Gross, and P. Argos. 1994. Intramolecular cavities in globular proteins. *Prot. Eng.* 7:613–626.

48. Hubbard, S. J., and P. Argos. 1996. A functional role for protein cavities in domain: domain motions. *J. Mol. Biol.* 261:289–300.

49. Carugo, O., and P. Argos. 1998. Accessibility to internal cavities and ligand binding sites monitored by protein crystallographic thermal factors. *Proteins*. 31:201–213.

50. Huber, R., R. Berendes, A. Burger, M. Schneider, A. Karshikov, H. Luecke, J. Römisch, and E. Paques. 1992. Crystal and molecular structure of human annexin V after refinement. Implications for structure, membrane binding and ion channel formation of the annexin family of proteins. *J. Mol. Biol.* 223:683–704.

51. Gerke, V., and S. E. Moss. 1997. Annexins and membrane dynamics. *Bioch. Biophys. Acta*. 1357:129–154.

52. Sopkova, J., M. Vincent, M. Takahashi, A. Lewit-Bentley, and J. Gallay. 1999. Conformational flexibility of domain III of annexin V at membrane/water interfaces. *Biochemistry*. 38:5447–5458.

53. Johansson, J. S., H. Zou, and J. W. Tanner. 1999. Bound volatile general anesthetics alter both local protein dynamics and global protein stability. *Anesthesiol*. 90:235–245.

54. Dilger, J. P., A. M. Vidal, H. I. Mody, and Y. Liu. 1994. Evidence for direct actions of general anesthetics on an ion channel protein. A new look at a unified mechanism of action. *Anesthesiol*. 81:431–442.

55. Pratt, M. B., S. S. Husain, K. W. Miller, and J. B. Cohen. 2000. Identification of sites of incorporation in the nicotinic acetylcholine receptor of a photoactivable general anesthetic. *J. Biol. Chem.* 275:29441–29451.

56. Nagele, P., L. B. Metz, and C. M. Crowder. 2004. Nitrous oxide (N_2O) requires the *N*-methyl-D-aspartate receptor for its action in *Caenorhabditis elegans*. *Proc. Natl. Acad. Sci. USA*. 101:8791–8796.

57. David, H. N., M. Ansseau, M. Lemaire, and J. H. Abraini. 2006. Nitrous oxide and xenon prevent amphetamine-induced carrier-mediated dopamine release in a memantine-like fashion and protect against behavioral sensitization. *Biol. Psychiatry*. 60:49–57.

58. Nagele, P., L. B. Metz, and C. M. Crowder. 2005. Xenon acts by inhibition of non-*N*-methyl-D-aspartate receptor-mediated glutamatergic neurotransmission in *Caenorhabditis elegans*. *Anesthesiol*. 103:508–513.

59. Peoples, R. W., C. Li, and F. F. Weight. 1996. Lipid vs protein theories of alcohol action in the nervous system. *Annu. Rev. Pharmacol. Toxicol.* 36:185–201.